THE JOURNAL OF BIOLOGICAL CHEMISTRY Vol. 276, No. 18, Issue of May 4, pp. 15337–15344, 2001
Printed in U.S.A.

Monitoring Agonist-induced Phospholipase C Activation in Live Cells by Fluorescence Resonance Energy Transfer*

Received for publication, August 8, 2000, and in revised form, December 15, 2000
Published, JBC Papers in Press, January 10, 2001, DOI 10.1074/jbc.M007194200

Jose van der Wal‡, Ron Habets‡§, Péter Várnai¶, Tamas Balla¶, and Kees Jalink‡‖

From the ‡Division of Cell Biology, The Netherlands Cancer Institute, Plesmanlaan 121, 1066CX Amsterdam, The Netherlands and the ¶Endocrinology and Reproduction Research Branch, National Institutes of Health, Bethesda, Maryland 20892-4510

Agonist-induced intracellular Ca^{2+} signals following phospholipase C (PLC) activation display a variety of patterns, including transient, sustained, and oscillatory behavior. These Ca^{2+} changes have been well characterized, but detailed kinetic analyses of PLC activation in single living cells is lacking, due to the absence of suitable indicators for use *in vivo*. Recently, green fluorescent protein-tagged pleckstrin homology domains have been employed to monitor PLC activation in single cells, based on (confocal) imaging of their fluorescence translocation from the membrane to the cytosol that occurs upon hydrolysis of phosphatidylinositol bisphosphate. Here we describe fluorescence resonance energy transfer between pleckstrin homology domains of PLCδ1 tagged with cyan and yellow fluorescent proteins as a sensitive readout of phosphatidylinositol bisphosphate metabolism for use both in cell populations and in single cells. Fluorescence resonance energy transfer requires significantly less excitation intensity, enabling prolonged and fast data acquisition without the cell damage that limits confocal experiments. It also allows experiments on motile or extremely flat cells, and can be scaled to record from cell populations as well as single neurites. Characterization of responses to various agonists by this method reveals that stimuli that elicit very similar Ca^{2+} mobilization responses can exhibit widely different kinetics of PLC activation, and that the latter appears to follow receptor activation more faithfully than the cytosolic Ca^{2+} transient.

One of the earliest effects of the addition of certain agonists to quiescent cells is a rapid increase in cytosolic free Ca^{2+} concentration ($[Ca^{2+}]_i$).[1] In most cases, these $[Ca^{2+}]_i$ increases are due to mobilization from internal Ca^{2+} stores, caused by activation of PLC enzymes that cleave phosphatidylinositol 4,5-bisphosphate ($PI(4,5)P_2$) in the plasma membrane to generate the second messengers inositol 1,4,5-trisphosphate (IP_3) and diacylglycerol. IP_3-mediated release of Ca^{2+} from internal endoplasmic reticulum stores has been well characterized, since the availability of specific vital dyes that allow monitoring of $[Ca^{2+}]_i$ in single living cells with high spatial and temporal resolution. These studies have demonstrated a variety of different response kinetics, including transient and sustained Ca^{2+} increases, oscillations and Ca^{2+} waves (1). An important conclusion drawn from these studies is that kinetic differences in $[Ca^{2+}]_i$ responses can have marked effects on downstream regulatory targets with important physiological consequences (2).

Although Ca^{2+} signals are believed to reflect IP_3 increases and hence PLC activation, it was noted in several studies that various agonists generate grossly different amounts of inositol phosphates, only to achieve similar $[Ca^{2+}]_i$ responses (3). However, due to the lack of suitable methods, activation and inactivation kinetics of PLC have not been characterized in single cells. An exciting recent development is the utilization of GFP-tagged protein domains for the *in vivo* visualization of inositide lipid dynamics. For example, the pleckstrin homology domain of PLCδ1 that binds to $PI(4,5)P_2$ has been used to monitor changes in the cellular levels of this lipid (4, 5) and the PH domains of Btk or PKB were employed to follow changes in 3-phosphorylated polyphosphoinositides (6, 7). In these studies detection is based on imaging of the change in localization of GFP-PH by fluorescence microscopy. PLCδ1PH-GFP, for instance, is located at the membrane in resting cells, where it is bound to $PI(4,5)P_2$ (5), and upon agonist-induced $PI(4,5)P_2$ hydrolysis it translocates to the cytosol. Subsequently, when $PI(4,5)P_2$ is resynthesized, fluorescence returns to the membrane. The transient translocation is usually detected in single cells by confocal imaging and quantified by post-acquisition image analysis (4, 6).

While this approach has a number of obvious advantages, including detection of changes in single living cells with time resolution in the second range, it also has several limitations. First, it is hard to obtain quantitative data from translocation studies using confocal microscopy. Even minor focal drift and changes in cell morphology, that often occur after stimulation, degrade signal-to-noise ratio, since these will render it difficult to reliably assign measurement regions (so-called regions of interest) that correspond to membrane and cytosol. Second, it is difficult to see translocation in very flat cells or in cellular subregions such as neurites and lamellipodia. Third, at fast imaging rates, confocal imaging requires high excitation intensities that can cause severe cell damage in a matter of minutes. Therefore, there is a trade-off between sampling speed and duration of the experiment. Moreover, single cell determinations are inherently variable, and the imaging approach is not easily extended to cell populations.

* The costs of publication of this article were defrayed in part by the payment of page charges. This article must therefore be hereby marked "*advertisement*" in accordance with 18 U.S.C. Section 1734 solely to indicate this fact.

‖ To whom correspondence should be addressed. Tel.: 31-20-512-1933; Fax: 31-20-512-1944; E-mail: kees@nki.nl.

§ Current address: Swammerdam Institute for Life Sciences, University of Amsterdam, Kruislaan 320, 1098SM Amsterdam.

[1] The abbreviations used are: $[Ca^{2+}]_i$, intracellular Ca^{2+}; $PI(4,5)P_2$, phosphatidylinositol 4,5-bisphosphate; IP_3, inositol 1,4,5-trisphosphate; FRET, fluorescence resonance energy transfer; BK, bradykinin; CFP, cyan fluorescent protein; CFP-PH, PLCδ1PH-CFP; FRAP, fluorescence recovery after photobleaching; GFP, green fluorescent protein; GFP-PH, PLCδ1PH-GFP; GPCR, G protein-coupled receptor; LPA, lysophosphatidic acid; NKA, neurokinin A; PLC, phospholipase C; PH, pleckstrin homology; YFP, yellow fluorescent protein; YFP-PH, PLCδ1PH-YFP.

To overcome these limitations, we have applied fluorescent resonance energy transfer (FRET) as a way to improve the detection of PH domain translocation. FRET, the radiationless transfer of energy from a fluorescent donor to a suitable acceptor fluorophore, depends on fluorophore spectral overlap and dipole alignment, and is a very steep function of donor-acceptor distance (for review, see Refs. 8 and 9). For the GFP mutants CFP and YFP, FRET can take place when the fluorophores are within ~10 nm distance. Here we describe FRET between CFP- and YFP-tagged PH domains of PLCδ1 as a sensitive readout for membrane localization that offers a number of the advantages over confocal imaging. FRET detects agonist-induced translocation of the fluorescent proteins from the membrane to the cytosol essentially identical to what was reported in GFP-PH imaging studies, without the need for optical sectioning, providing with a more reliable quantitative measurement of membrane localization. In addition, this method is applicable for cell populations and single neurites, and allows analysis for extended periods of time with minimal cell damage. Comparison of FRET responses in several cell types with various agonists reveals significant differences between kinetics of PLC activation triggered via various GPCRs, despite similar $[Ca^{2+}]_i$ responses. It is also shown that receptor activity and desensitization, rather than post-G protein mechanism(s) is a major determinant of the PLC activation pattern.

EXPERIMENTAL PROCEDURES

Materials—1-Oleoyl-LPA, histamine, bradykinin, phenylarsine oxide, and quercetin were from Sigma; neurokinin A, caged IP_3 (catalog number 407135), and ionomycin were from Calbiochem-Novabiochem Corp. (La Jolla, CA); *myo*-[^{3}H]inositol (60 Ci/mmol) was from Amersham Pharmacia Biotech. Fura red (K salt) and bodipy-FL were from Molecular Probes Inc. (Eugene, OR). All other chemicals were of analytical grade.

DNA Constructs—The pleckstrin homology domain was obtained from the Superhiro PLCδ1PH construct (amino acids 1–174; a kind gift from Dr. Tobias Meyer) and cloned into the eukaryotic expression vector pECFP-C1 (CLONTECH, CA). Two primers (PLCδPH1; 5′-CCTGCGGCCGCGGTACCGATATCAGATGTTGAGCTCCTTCAG-3′ and PLCδPH2; 5′-CCGAATTCCCGGGTCTCAGCCATGGACTCGGGCCGGGACTTC-3′) were designed to generate the PH domain in-frame behind the CFP followed by a stop codon. The polymerase chain reaction product was cloned into the pECFP plasmid with the restriction sites *Eco*RI and *Eco*RV on *Eco*RI and *Sma*I, leading to pECFP-PH.

YFP was obtained from yellow Cameleon 2.0 (a kind gift from A. Miyawaki and R. Tsien) and subcloned into cloning vector PGEM3z (Promega), via *Sac*I and *Eco*RI, and subsequently into pcDNA3 (Invitrogen) via *Bam*HI and *Eco*RI. Polymerase chain reaction on YFP-pcDNA-3 with primers T7 (Promega) and GFP3; 5′-GGCTGAGACCCGGGAATTCGGCTTGTACAGCTCGTCCATG-3′ was done to remove the stop codon. The polymerase chain reaction product, taken between primers PLCδPH1 and PLCδPH2, was cloned in-frame behind YFP with *Eco*RI and *Not*I, leading to pcDNA3YFPPH. To obtain pcDNA3eGFPPH, YFP was swapped with enhanced GFP, using primers T7 and GFP3 on pcDNA3eGFP and restriction enzymes *Bam*HI and *Eco*RI.

For YFP-CAA*X* and GFP-CAA*X*, the membrane localization sequence of K-Ras (KMSKDGKKKKKKSKTKCVIM) was obtained by polymerase chain reaction amplification from Bp180-CAAX (GenBank™ accession numbers M54968 and M38506), using primers CAA*X*3 5′-CCGAATTCCCGGGTCAAGATGAGCAAAGATGGTAAAAAG-3′, containing an *Eco*RI site, and CAAX2; 5′-CCTGCGGCCGCGGTACCGAGATCTTTACATAATTACACACTT-3′, that contained a *Not*I site behind the stop codon. The final constructs were made by exchanging the PH domain from YFP-PH and GFP-PH for the CAA*X* domain using *Eco*RI and *Not*I. All clones were verified by sequence analysis. YFP-CAA*X* contained a point mutation (Val instead of Gly in the CAA*X* domain), but this did not influence its membrane localization. The constitutively active mutants of $G\alpha_q$ and $G\alpha_{12}$ cloned into pcDNA3 vectors were a kind gift from Dr. O. Kranenburg *et al.* (10).

Cell Culture and Transfections—N1E-115 neuroblastoma cells were seeded in 6-well plates at ~25,000 cells per well on 25-mm glass coverslips, and cultured in 3 ml of Dulbecco's modified Eagle's medium supplemented with 10% fetal calf serum and antibiotics. Unless otherwise indicated, constructs were transfected for 6–12 h using calcium phosphate precipitate, at 0.8 μg of DNA/well. Following transfection, cells were incubated in serum-free Dulbecco's modified Eagle's medium for 12–48 h. For fluorescence detections, coverslips with cells were transferred to a culture chamber and mounted on an inverted microscope. All experiments were performed in bicarbonate-buffered saline (containing, in mM, 140 NaCl, 5 KCl, 1 $MgCl_2$, 1 $CaCl_2$, 10 glucose, with 10 mM HEPES added), pH 7.2, kept under 5% CO_2, at 37 °C.

Inositol Phosphate Determinations—Preparation, culture, and labeling of bovine adrenal glomerulosa cells have been described elsewhere (11). Cells labeled with *myo*-[^{3}H]inositol for 24–48 h were stimulated by angiotensin II (30 nM) for the indicated times in a medium containing either Sr^{2+} or Ca^{2+}. Reactions were terminated with perchloric acid and inositol phosphates were separated by high performance liquid chromatography essentially as described previously (11).

Confocal Microscopy and Image Analysis—For confocal imaging, a Leica DM-IRBE inverted microscope fitted with a TCS-SP scanhead was used. Excitation of enhanced GFP was with the 488-nm argon ion laserline, and emission was collected at 500–565 nm. For translocation studies, series of confocal images were taken at 2–10-s intervals and stored on disc. Determination of the ratio of membrane to cytosolic fluorescence by directly assigning regions of interest for membrane and cytosol was hampered by the shape changes of cells during experiments (see text). Using Qwin software (Leica) this ratio was therefore calculated by post-acquisition automated regions of interest assignment and analysis. In brief, a binary mask of the transfected cell was lined out using a thresholding step on a smoothed image. From this mask, the area corresponding to the membrane was eroded by a user-selectable amount to delineate the membrane. Further erosion was then applied to reliably separate membrane from cytosol area, and the remaining area was taken to represent cytosol. This mask was updated for each image in a series, and translocation was expressed as ratio of the fluorescence values for membrane and cytosol area, to correct for bleaching. This approach corrects fully for cell movements and shape changes, and was able to reliably detect very minor translocations (using *e.g.* diluted agonists) that went unnoticed for the eye.

Fluorescence Determinations—For FRET experiments, cells on coverslips were placed on an inverted Zeiss Axiovert 135 microscope equipped with a dry Achroplan ×63 (NA 0.75) objective. Excitation of CFP was at 425 ± 5 nm, and emission was collected with a 460-nm dichroic mirror. Emission of CFP and YFP was split using an additional 505-nm dichroic mirror and filtered with 475DF30 and 540DF40 band pass filters, respectively. Detection was with PTI model 612 analog photomultipliers, and for data acquisition, the FELIX software (PTI Inc.) was used. FRET was expressed as ratio of CFP to YFP signals, the value of which was set as 1.0 at the onset of the experiment. Changes are expressed as percent deviation from this initial value of 1.0. For detection of intracellular Ca^{2+}, Yellow Cameleon 2.1 was used (12) at the same wavelengths.

For sustained stimulation, agonists and inhibitors were added to the medium from concentrated stocks. Stimulation with short pulses of NKA was performed by placing a glass micropipette (tip Ø ~2 μm) at about 25 μm from the cell using an Eppendorf microinjection system and applying pulses of pressure for 10 s. It was verified using Lucifer Yellow in the pipette that following termination of the pressure pulse the concentration at the cell rapidly dropped toward zero.

Loading and Flash Photolysis of Caged IP_3—Before electroporation, adherent cells grown on coverslips were washed twice in intracellular buffer (containing in mM: 70 KCl, 70 K glutamate, 2 $MgCl_2$, 0 $CaCl_2$, 5 phosphate buffer, pH 7.1) and then 70 μl of this intracellular buffer was added to the cells with 20 μM Fura red tetrapotassium salt and 1, 10, or 100 μM caged IP_3. Electroporation was achieved by a series of 15 high frequency square wave pulses, (1-s spaced, amplitude 150 V, frequency 80 kHz, lasting 0.5 ms each) using 2 platina electrodes of 8 × 3 mm with 2.5-mm spacing. The efficiency of this method was assessed by control permeabilizations that were performed on the stage of a confocal microscope. This protocol caused complete permeabilization (based on equilibration of intracellular calcein concentrations with the extracellular buffer) of the cells in the area between the electrodes.

For photorelease of caged IP_3, a single cell was illuminated with a short pulse of UV light (340–410 nm) from a 100 W HBO lamp using a shutter. The shutter open time was adjusted to give full release of caged IP_3, that is no response being observed with a subsequent illumination. For partial photolysis, the flash intensity was adjusted by neutral density filters placed in the illumination pathway.

Quantitation of Expression Levels—For quantitation of expression levels of CFP-PH and YFP-PH, cellular fluorescence was compared with the fluorescence of a solution of known concentration of purified, bac-

terially expressed CFP-PH or YFP-PH, following the method of Miyawaki *et al.* (37). In short, CFP-PH and YFP-PH were expressed as glutathione *S*-transferase fusion proteins, and purified on glutathione-Sepharose beads. Protein concentration (5.4 μM) was measured by the BCA Protein Assay (Pierce). Calibration of the fluorescent brightness of this protein preparation, using values for molar absorption and quantum yield of 36,500 and 0.63, respectively (13), against commercial standards indicated that essentially 100% of proteins were fluorescent. The solution was then introduced in a linear wedge-shaped chamber (0–170 μm thickness) that was placed on the microscope (using NA 0.7 objective), and the position of the chamber was adjusted to give a fluorescence readout that matched that of a single, CFP or YFP expressing cell. The estimate of the fluorescent protein concentration in the cell was obtained by comparing the local thickness of the wedge to that of an average cell (17 μm). Relative amounts of CFP-PH and YFP-PH expression in cells were always determined under conditions of full cytosolic localization of the constructs. Comparison of voxel intensities within cells and the protein solution using a confocal microscope gave very similar results.

At the onset of each experiment, photomultiplier gains (high voltage) were adjusted to give a standard 6 V output for the resting cell. Noting that over an extended range of light input, every 2-fold change in intensity corresponds to a 35 V change in cathode voltage, cell intensities were measured. By comparing these intensities to the values obtained with the GFP wedge, estimates of expression levels were obtained.

Fluorescence Recovery after Photobleaching (FRAP)—For FRAP experiments, cells were imaged using a Leica TCS-SP confocal microscope equipped with ×63 (NA 1.3) oil immersion objective. The beam from a external ArKr laser (25 mW) was coupled into the backfocal plane of the objective via the epifluorescence excitation port, using a 30/70 beamsplitter, thus allowing simultaneous imaging and spot bleaching. Spots of ~1.3 μm (full width half-maximum) were bleached (>95%) in the basal membrane using a single 30-ms pulse from the ArKr laser during data collection in linescan mode at 1000, 500, or 125 Hz. Data were corrected for slight (<7%) background bleaching and fitted with single exponents using Clampfit software (Axon Instruments).

RESULTS AND DISCUSSION

Fluorescence Resonance Energy Transfer between Plasma Membrane-localized PLCδ1PH-CFP and PLCδ1PH-YFP—PH-CFP and PH-YFP chimera were transiently transfected into N1E-115 mouse neuroblastoma cells at a 1:1 molar ratio. After 1–2 days, cells were transferred to an inverted epifluorescence microscope and assayed for FRET by simultaneously monitoring the emission of CFP (475 ± 15 nm) and of YFP (530 ± 20 nm), while exciting CFP at 425 ± 5 nm. In resting cells, PH-CFP and PH-YFP reside at the plasma membrane bound to $PI(4,5)P_2$, and the two fluorophores remain within resonance distance. Upon activation of PLC by the addition of BK, $PI(4,5)P_2$ is rapidly hydrolyzed and consequently PH domains can no longer bind to the plasma membrane. The distance(s) between fluorophores increase significantly, and therefore FRET no longer occurs (Fig. 1). As a result, the donor (CFP) emission intensity increases, while the acceptor (YFP) emission decreases. By taking the ratio of CFP to YFP emission, the FRET signal becomes essentially independent on excitation intensity fluctuations and photobleaching.

The kinetics of BK-induced PLC activation in N1E-115 cells as detected by FRET is characterized by a rapid onset, with translocation peaking at 20–30 s after addition of the agonist. The decaying phase is somewhat slower, usually returning to baseline within 1 to 4 min. This time course is very similar to that deduced from confocal detection of PLCδ1PH-GFP translocation recorded under identical conditions (Fig. 1*C*). In this latter case, the data were extracted from a time series using post-acquisition automated image analysis (see "Experimental Procedures"). Similar translocation responses can be obtained by FRET in other cell types, including A431 epidermoid carcinoma cells, HEK293 embryonal kidney cells, and COS monkey kidney cells stimulated with a variety of ligands to G_q-coupled receptors.

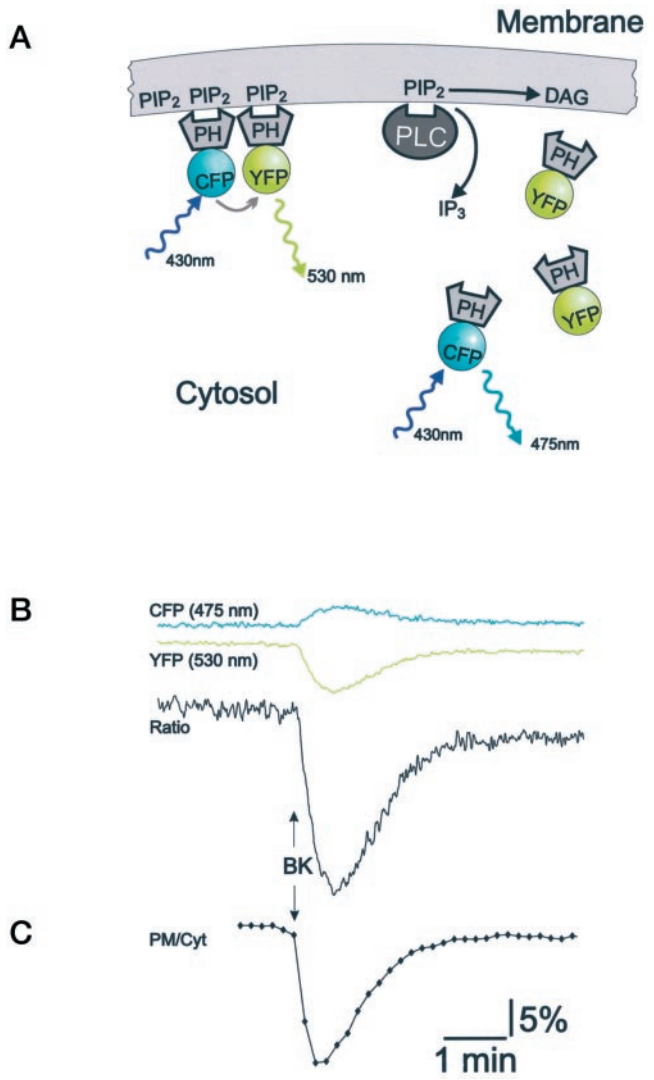

FIG. 1. **Fluorescence resonance detection of PH domain translocation.** *A*, schematic representation of FRET occurring between CFP-PH and YFP-PH bound to the membrane. Upon hydrolysis of $PI(4,5)P_2$, PH domains translocate to the cytosol and FRET ceases. *B*, emission signals of CFP and YFP collected at 475 and 530 nm respectively, and their ratio (530/475), recorded from a single N1E-115 cell stimulated with bradykinin (BK, 1 μM). Signals were low-pass filtered at 2 Hz and sampled at 3 Hz. *Scale bar* for ratio signal shows percent deviation from baseline. *C*, confocal detection of GFP-PH translocation, depicted on the same scale. Images were collected once per 10 s, and the ratio of fluorescence intensities in membrane and cytosol (*PM/Cyt*) was deduced for each image by post-acquisition automated image analysis (see "Experimental Procedures" for details).

The above described kinetics with a fast and rather complete translocation induced by BK, suggest that $PI(4,5)P_2$ depletion after stimulation is quite extensive. While most reports of agonist-induced $PI(4,5)P_2$ hydrolysis, as detected biochemically from [^{3}H]inositol-labeled cells, show slower and less pronounced decreases in phosphoinositide levels, considerable agonist- and cell type-dependent variations exist, *e.g.* Refs. 14–16. Where early time points were also studied, rapid decreases in $PI(4,5)P_2$ levels have been detected (17–19). For example, significant bradykinin-induced $PI(4,5)P_2$ decreases were reported to occur within 10 s in bovine aortic endothelial cells (20), and at 1 min in bombesin-stimulated 3T3 cells (18). Rapid recovery toward basal levels has also been found. Wijelath *et al.* (17) reported as much as 85% hydrolysis of $PI(4,5)P_2$ at 5 s after stimulation of macrophages with interleukin, while $PI(4,5)P_2$ levels recovered to 50% at 60 s. Similar fast recovery was also

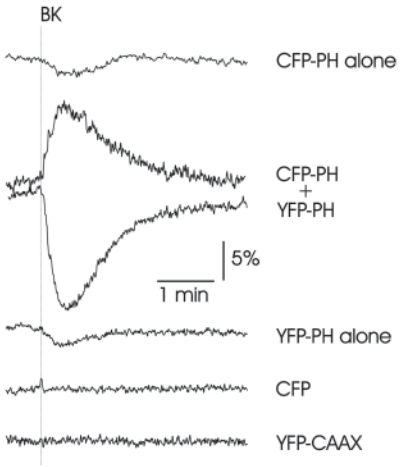

FIG. 2. **Characterization of fluorescence emission.** Cells expressing the constructs as indicated were stimulated with 1 μM bradykinin and fluorescence emission was detected at the indicated wavelength. See the text for further details.

seen in other cell types (18, 19). Since biochemical analyses have to rely upon measurements on cell populations, where not all cells give synchronized and identical responses (and many cells may not respond at all), it is not surprising to find differences between the results of measurements with these two alternative approaches.

Characterization of Fluorescence Signals—During agonist-induced translocation, several factors may affect the fluorescent properties of these PH domain chimeras as well as the transfer of fluorescent energy between them (21). For example, the move away from a compartment adjacent to the lipophilic membrane could alter fluorescent characteristics, and is also likely to alter FRET by increasing the degree of rotational freedom. While the relative influence of increased rotational freedom on the translocation-induced decrease in FRET is difficult to assess in this model sytem, we analyzed fluorescence changes in some further detail. Cells were transfected with only one of the PLCδ1PH-CFP or PLCδ1PH-YFP constructs. After stimulation, a small but consistent transient fluorescence decrease was observed with either the CFP or the YFP-tagged PH domains (Fig. 2). The original green construct (PLCδ1PH-GFP) displayed similar behavior (not shown). This transient decrease is likely caused by fluorophore displacement from the membrane, since it is not observed in cells that express a more stably membrane-anchored GFP-CAA*X*, nor is it seen in cells that express a mutated PLCδ1PH-GFP (R40L) (5) that cannot bind $PI(4,5)P_2$ and, therefore, is cytosolic throughout the experiment. The precise mechanism that causes this decrease of emission upon cytosolic translocation is unknown; however, influence of the local microenvironment (*e.g.* hydrophobicity, charged groups, changing ion concentrations etc.) on the spectral properties of GFP seems to be the likely reason (21). When recording FRET, this downward "displacement" effect will be added to the translocation-induced decrease of the YFP signal, while it will lessen the simultaneous CFP increase, likely explaining why the translocation-induced decrease in YFP signal is somewhat larger than the increase in CFP fluorescence. However, expressing FRET as an emission ratio largely eliminates this effect. As expected, FRET could also be measured in cells that coexpress PLCδ1PH-CFP with YFP-CAA*X* (not shown); however, using this pair, ratioing does not cancel the above mentioned displacement effect.

To assess the effects of construct concentrations on FRET, we compared cells expressing various levels of the chimeric proteins. Intracellular fluorescent protein concentrations were estimated by comparing the emission intensities of individual cells to those of a solution of bacterially expressed, purified protein of known concentration (37) (see "Experimental Procedures"). Based on these estimates, resonance could be observed in cells with expression levels between about 0.8 and 80 μM, over a 100-fold concentration range. However, FRET was not observed in cells expressing less than ~400 nM of each of the constructs. High expression levels, on the other hand, appeared to be detrimental to the cells (as judged from the appearance of membrane blebs, rounding and detachment of cells 2–3 days after transfection). For our analysis, we selected cells with estimated expression levels between 0.8 and 12 μM**,** which corresponds to the range that is used for confocal detection of translocation, the lower value being just 2 to 3 times the autofluorescence of the cells (13). These data also revealed that PLCδ1PH-CFP expression levels (detected in fully translocated cells) did not differ more than about 2-fold from those of PLCδ1PH-YFP in most cells. It is interesting to note that we could not see signs of saturation of the membrane-binding sites for the fluorescent PH domains, and could not establish a trend in which higher PH domain expression would be associated with altered translocation kinetics. Whether cells respond to the expression of these probes with compensatory increases in $PI(4,5)P_2$ levels remains to be investigated. Nevertheless, possible interference of the expressed PH domains with cellular signals including PLC activation *per se*, needs to be kept in mind when using such analyses.

Can such estimates of CFP and YFP concentrations be used to calculate lipid concentrations and molecular proximity in the cells studied? If we model a typical attached N1E-115 cell with a pyramid of 20 × 20-μm base and 10-μm height (having 1.3 pl volume and 1100 μm^2 surface), and assume that (i) the concentration of both chimera is 10 μM; (ii) 50% of fluorophores are located at the membrane (complete translocation roughly doubles the fluorescence in the cytosol); (iii) the distribution of fluorophores is homogenous along the membrane; and (iv) fluorophores are insensitive to the local environment, then the calculated mean distance between fluorophores is about 10 nm, which is close to the reported Forster radius (50 Å) for FRET between this pair of fluorophores (21). However, it should be emphasized that these assumptions are valid only as first approximations. For example, we and others (22) have noted that GFP-PH is not homogeneously localized along the plasma membrane. Also, as discussed above, the spectral properties of the fluorescent proteins are sensitive to the microenvironment. Nevertheless, these data set a lower limit for the density of $PI(4,5)P_2$ molecules available for PH binding at the inner surface of the plasma membrane.

GFP-PH Rapidly Shuttles between Membrane and Cytosol—Another important characteristic we wanted to address was membrane association and dissociation rates of the PH chimera. These rates directly influence reliability of FRET in reporting rapid changes in PLC activity, and are also relevant to the ability of PLC to hydrolyze $PI(4,5)P_2$ in cells that express high levels of the PLCδ1PH-GFP protein. We, therefore, performed FRAP experiments to estimate the binding and dissociation kinetics of PLCδ1PH-GFP in the membrane. Fig. 3 shows representative results from such FRAP experiments in N1E-115 cells. In *panels A* and *B*, the recovery rates are depicted for GFP-CAA*X* and PLCδ1PH(R40L)-GFP, constructs that are delimited to the plasma membrane and the cytosol, respectively. The former presents the extreme of slow, purely membrane-delimited diffusion (2.81 ± 0.31 s, n = 15), and the latter of fast cytosolic diffusion (0.201 ± 0.022 s, n = 15). Since FRAP of membrane-localized PLCδ1PH-GFP is significantly faster than that of the membrane-delimited GFP-CAA*X*

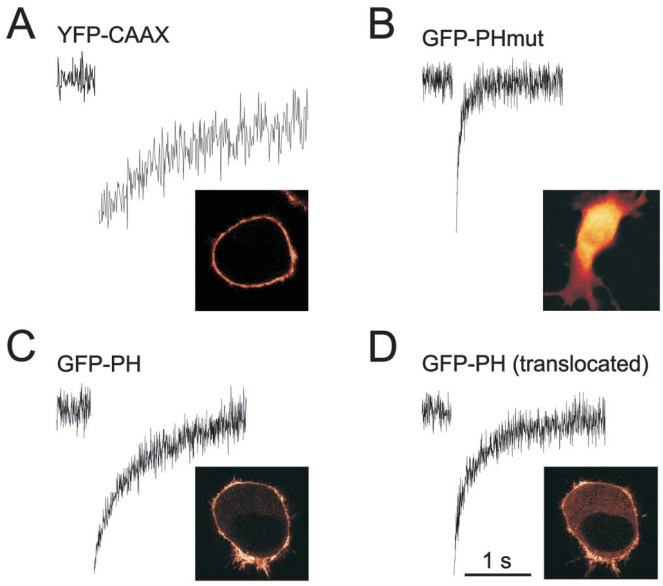

FIG. 3. **FRAP reveals dynamic movements of GFP-PH between cytosol and membrane.** Spots (~1.3 μm full-width half maximum) were completely bleached in the basal membrane (or in the cytosol for *B*) with a 30-ms pulse of 488 nm laser light, and recovery was monitored in line scan mode in a confocal microscope. FRAP of membrane-delimited YFP-CAA*X* (*A*); cytosolic PLCδ1PH(R40L)-GFP mutant that cannot bind $PI(4,5)P_2$ (*B*); PLCδ1PH-GFP in a resting cell (*C*); and PLCδ1PH-GFP in a cell that has agonist-induced partial translocation of fluorescence (*D*). *Insets* show confocal images for the distribution of these constructs, taken from representative cells.

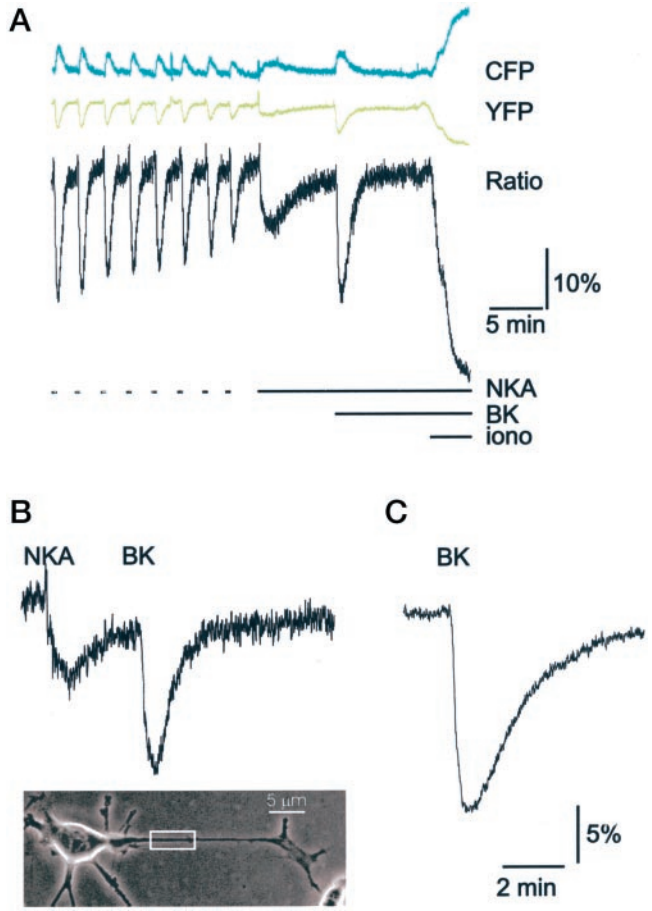

FIG. 4. **Using FRET to record PLC activation in single cells, neurites, or in cell populations.** *A,* a single N1E-115 cell was stimulated repeatedly with NKA as indicated by the *lines* (*dashes*, 10-s pulses of 100 μM NKA from a puffer pipette; *solid line*, addition of 1 μM final concentration to the culture dish). The response indicates repeated PLC activation, detected as decreases in FRET, and exhibits partial desensitization. Translocation induced by subsequently added BK (1 μM) was not desensitized by NKA pretreatment. For calibration, maximal translocation was induced by adding 5 μm ionomycin + 2 mM extra Ca^{2+} (5). *B,* FRET recording from a single neurite of a neuroblastoma cell, differentiated by culturing in serum-free medium for 48 h. Area of measurement (3.5 × 9 μm) is indicated in the micrograph. For this experiment, excitation bandwidth was increased to 20 nm. *C,* FRET recording from a cluster of about 15 transfected cells demonstrates improved signal-to-noise ratio and averaged kinetics (note the same scale for *B* and *C*).

(1.22 ± 0.23 s, $n = 40$; $p < 0.005$; compare *panels A* and *C*), its recovery has to be partially through the cytoplasma. Thus, $PI(4,5)P_2$-PH binding is a dynamic process, with on-off rates in the order of seconds. In support of this notion, FRAP further decreased during agonist-induced partial translocation, when association rates are increased due to the raised cytosolic GFP-PH levels (*panel D*). The rapid shuttling between membrane and cytosol of individual PLCδ1PH-GFP molecules could explain why $PI(4,5)P_2$ is still available for PLC-mediated hydrolysis or for binding of other proteins in cells expressing these chimeras.

Widefield FRET Detection Allows Prolonged Monitoring Independent of Cell Shape Changes—Rapid confocal scanning of cells transfected with PLCδ1PH-GFP leads to severe phototoxic damage (often within 100 frames), manifested as membrane blebbing and loss of membrane integrity within minutes. Using wide field optical detection and integrating emission from an entire cell (or even clusters of cells) allowed excitation intensity to be dimmed by as much as 100 to >1000-fold, while still retaining acceptable signal-to-noise ratio. Thus, FRET can be followed in single cells for extended periods of time without detectable cell damage. This permits recording of complex stimulation protocols, as shown in Fig. 4*A*. Here, a trace obtained from a single N1E-115 cell that is repeatedly stimulated with short pulses of neurokinin A (NKA) from a puffer pipette indicates repeated PLC activation. The response to NKA displays incremental partial homologous desensitization of PLC activation, while the response to subsequently added BK is unaltered. Optimizing for low excitation intensity, recordings of several hours can be obtained with sub-second resolution.

In N1E-115 and other cells, addition of certain agonists causes rapid and significant shape changes. For instance, LPA causes neurites to retract and the cell soma to round up within 60 s (23). In contrast, addition of BK has opposite effects, promoting a differentiated phenotype (24). During confocal imaging, such shape changes (as well as the slight drift in focal plane that inevitably occurs over prolonged times) seriously complicate the quantification of GFP-PH translocation. Since our FRET analysis uses the total integrated emission from a cell, shape changes and focal drift do not present any problems.

In very flat and small cell structures such as neurites and lamellipodia (below ~2 μm in thickness), confocal imaging cannot detect translocation due to its inherent limit in *z* axis resolution. However, in such cases changes in FRET can still be reliably detected as shown by the agonist-induced PLC activation recorded over a single neurite (Fig. 4*B*). FRET can also be recorded from cell populations (Fig. 4*C*) providing with an average response that would need analysis of hundreds of single cell recordings. Thus, detecting resonance between fluorescent protein-labeled PH domains has several advantages to report on the distribution of PH domains without the need for confocal detection.

Does FRET Report Changes in Membrane $PI(4,5)P_2$ or Increases in Cytosolic IP_3?—While PLCδ1PH-GFP has been introduced as an indicator of membrane $PI(4,5)P_2$ (4, 5), it also displays high affinity to IP_3 (25), which may significantly ex-

ceed its affinity to $PI(4,5)P_2$, although it is difficult to accurately measure the latter as it is displayed *in vivo*. Based on such relative affinity estimates, Hirose and co-workers (25) recently suggested that PLCδ1PH-GFP actually monitors IP_3 increases rather than the changes in lipid levels in Madin-Darby canine kidney cells. They reported that microinjection of IP_3 in Madin-Darby canine kidney cells was sufficient to cause displacement of PLCδ1PH-GFP from the membrane to the cytosol through competition for binding of the fluorescent construct to membrane $PI(4,5)P_2$. They also showed that expression of an IP_3 5-phosphatase completely blocked the agonist-induced translocation of the fluorescent protein and concluded that $PI(4,5)P_2$ changes do not make a significant contribution to the translocation response during stimulation.

While FRET analysis effectively monitors the result of PLC activation regardless of whether it is the lipid decrease or the IP_3 increase that is more important for the translocation response, we felt that this question deserves a more detailed analysis. First we wanted to determine whether intracellular applications of IP_3 that generate a Ca^{2+} signal comparable to that evoked by an agonist would cause translocation of the PLCδ1PH that is similar to what is caused by agonist stimulation. N1E-115 cells were loaded with 20 μM of the calcium indicator Fura red and 100 μM caged IP_3 by *in situ* high frequency electroporation. Unlike microinjection, this technique allows setting of the final concentration of caged IP_3 in the cytosol with high precision (see "Experimental Procedures"), as confirmed by the observation that upon electroporation, intracellular and extracellular fluorescence levels were equal. As shown in Fig. 5*A*, UV flash photolysis of 1 μM caged IP_3 rapidly mobilized Ca^{2+} from internal stores, with no visible translocation of PLCδ1PH-GFP to the cytosol. Subsequent release of 10 μM caged IP_3 caused a higher Ca^{2+} response and a small translocation. Only high IP_3 concentrations that evoked a large and prolonged Ca^{2+} increase were able to displace PLCδ1PH-GFP from the plasma membrane. In contrast, BK stimulation caused a larger translocation response than the highest amounts of IP_3 with a Ca^{2+} signal that was comparable to that induced by the smallest amount of IP_3 (Fig. 5*A*). In cells electroporated with no caged IP_3 in the electroporation buffer, intense UV flashes did not influence intracellular Ca^{2+} levels, membrane localization of the chimera, or any of the BK-induced changes herein (not shown).

Next, the effects of interfering with $PI(4,5)P_2$ resynthesis on the kinetics of translocation in N1E-115 cells was studied. $PI(4,5)P_2$ resynthesis was inhibited by low concentrations (5 μM) of phenylarsine oxide (Fig. 5*B*) or quercetin (26), or by depletion of free inositol using prolonged incubation in inositol-free medium (not shown). In phenylarsine oxide-treated cells, BK induced a sustained translocation of PLCδ1PH-GFP to the cytosol, while IP_3 increases in such cells are only transient (27). In control experiments, these pretreatments did not influence signaling events such as BK-induced Ca^{2+} signaling (peak Ca^{2+} values of 870 ± 130 nM in control cells, and 845 ± 114 nM, in phenylarsine oxide-pretreated cells, $n = 6$, mean ± S.E.) or the thrombin- and lysophosphatidate-induced actinomyosin contraction (23, 28). Similar observations were made in HEK293 cells (not shown), suggesting that the translocation of PH domains under these conditions reports the depleted $PI(4,5)P_2$ pool rather than the transient IP_3 increase.

Moreover, when adrenal glomerulosa cells were stimulated with angiotensin II in the presence of Sr^{2+}, a condition under which IP_3 metabolism via $Ins(1,3,4,5)P_4$ is greatly reduced (11), hence yielding significantly higher $Ins(1,4,5)P_3$- and diminished $Ins(1,3,4)P_3$ increases (Fig. 5, *C* and *D*), the translocation of PLCδ1PH-GFP was not significantly different (Fig. 5*E*) from

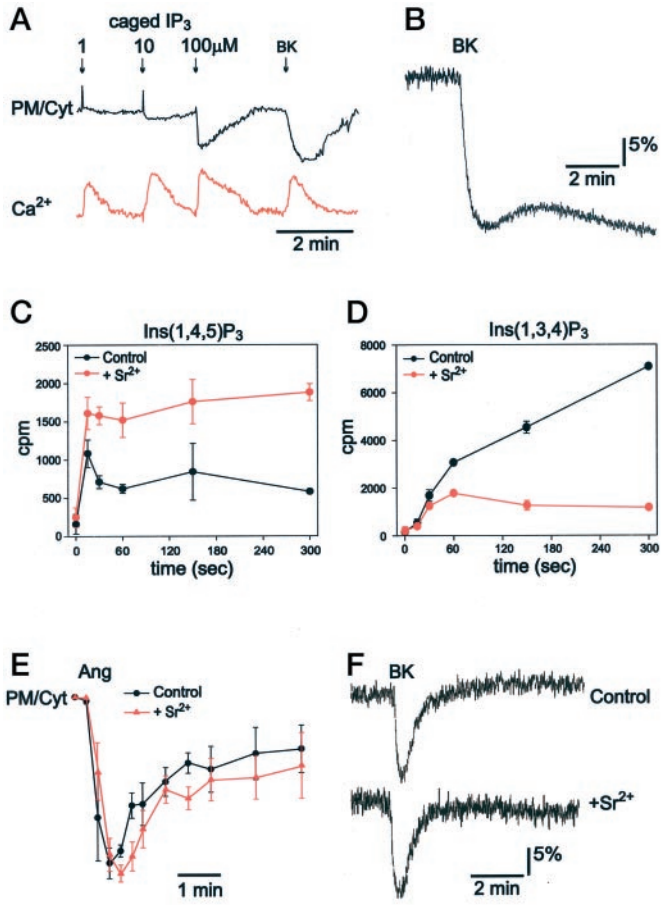

FIG. 5. **The PH domain of PLCδ1 reports changes in $PI(4,5)P_2$ rather than in IP_3.** *A*, cells expressing GFP-PH were loaded with both Fura red (20 μM) and caged IP_3 (100 μM) by *in situ* high frequency electroporation. Shown is the response of a single cell, assayed simultaneously for GFP translocation and Ca^{2+} mobilization induced by flash photolysis of caged IP_3. *Arrows* indicate photolysis of 1, 10, and 90 μM as detailed under the "Results." For comparison, bradykinin (1 μM) was added afterward. Representative trace from 16 similar experiments. *B*, FRET response to bradykinin detected in a single cell, pretreated with 5 μM phenylarsine oxide for 10 min. *C* and *D*, time course of $Ins(1,4,5)P_3$ and $Ins(1,3,4)P_3$ formation in adrenal glomerulosa cells prelabeled with [^{3}H]inositol, after stimulation with angiotensin II (*Ang*, 1 μM) in the presence of 2 mM Sr^{2+} (*red*) or Ca^{2+} (*black*). *E*, angiotensin II-induced translocation as quantitated by analysis of serial confocal images of glomerulosa cells in the presence of Sr^{2+} (*red*) or Ca^{2+} (*black*). Data points represent mean ± S.E., $n = 5$. *F*, bradykinin-induced translocation, with and without Sr^{2+}, as detected by FRET in N1E-115 cells.

that observed in the presence of Ca^{2+}. Translocation responses of N1E-115 cells in response to BK were also similar in the presence of Ca^{2+} or Sr^{2+} (Fig. 5*F*).

Taking all these data together, we conclude that, at least for the cells and agonists tested in the present study, PLCδ1PH-GFP translocation primarily reports changes in membrane $PI(4,5)P_2$ content and not the IP_3 increases. The reason for the apparently stronger binding of PLCδ1PH to membranes observed in live cells compared with the reported low *in vitro* affinity (25) to $PI(4,5)P_2$ containing lipid vesicles or BiaCore surface (29), is unclear at present, but may indicate a more complex interaction of the PLCδ1PH domain with the native membranes that is not mimicked by the *in vitro* experiments. However, we did confirm the finding (25) that high IP_3 levels can make significant contributions to the translocation response. Whether such high levels or IP_3 occur under the experimental conditions used with intact cells remains to be elucidated. Nevertheless, possible interference from large IP_3

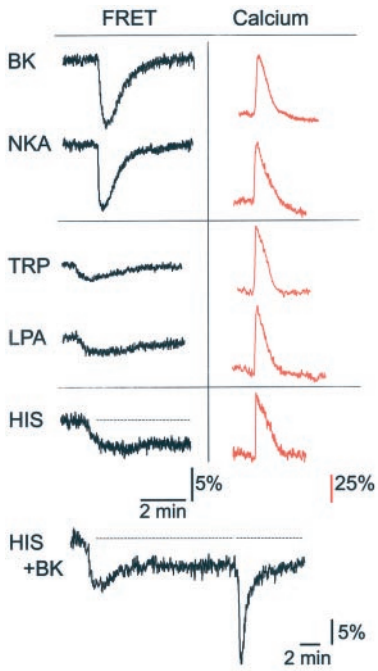

FIG. 6. **Heterogeneity of translocation responses to different GPCR agonists.** Single N1E-115 cells expressing CFP-PH and YFP-PH were stimulated with 1 μM BK, 1 μM NKA, 50 μM thrombin-receptor activating peptide (*TRP*), 1 μM LPA, or 10 μM histamine (*HIS*). In *black*, PLC activation as assayed by FRET. In *red*, intracellular Ca^{2+} recordings for these agonists detected ratiometrically using Yellow Cameleon 2.1 in separate experiments. Changes in fluorescence ratio are expressed as percentage of resting values. Shown are representative examples of experiments performed at least 10 times.

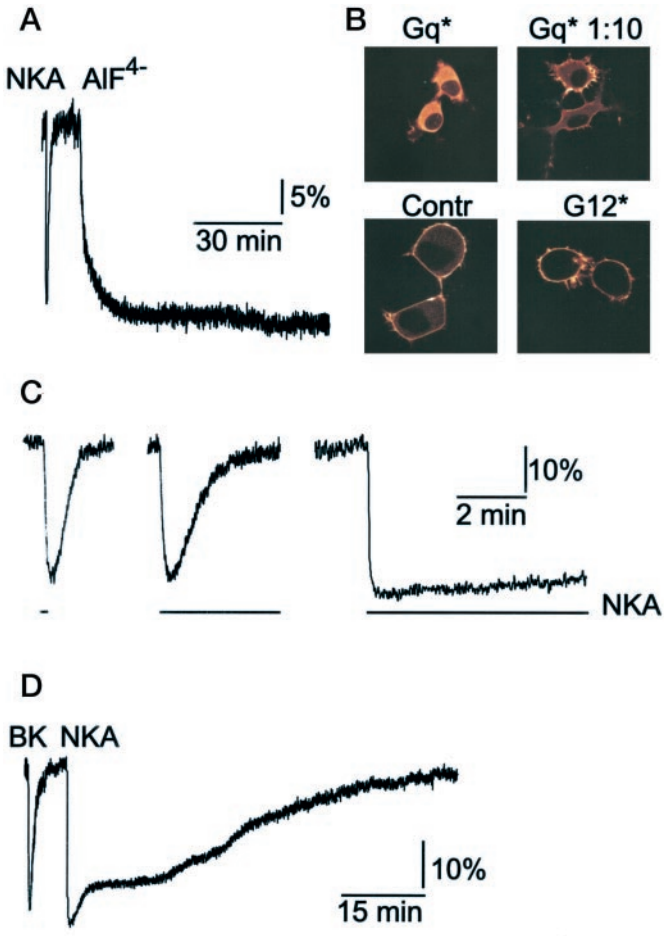

FIG. 7. **FRET inactivation kinetics mirror receptor inactivation.** *A*, FRET recording from a single N1E-115 cell stimulated with 1 μM NKA or 1 mM aluminum fluoride (AlF^{4-}). *B*, confocal micrographs of cells taken 56 h after transfection with PLCδ1PH-GFP (5 μg of DNA/well) together with different amounts of constitutively active $G\alpha_q$ subunit (*Gq**, 0.8 μg/well, and *Gq* 1:10*, 0.08 μg/well) or with constitutively active $G\alpha_{12}$ at 0.8 μg/well (*G12**). *C*, PLC activation, as detected by FRET, in a single neuroblastoma cells (*left panel*) that expresses wild-type NKA receptors, stimulated with 10-s pulse from a puffer pipette with 100 μM NKA; and cells stimulated by prolonged addition of NKA (1 μM) to the medium, expressing either wild-type receptors (*middle panel*) or a mutant, truncated at its C terminus (33) (*right panel*). Recordings are all to the same scale. *D*, kinetics of FRET after NKA addition in a N1E-115 cell transfected with the C-terminal truncated NK2 receptors on an extended time scale.

increases should be kept in mind during interpretations of the results of such translocation experiments.

FRET Reveals Response Heterogeneity to Different GPCR Agonists That Is Not Reflected in Ca^{2+} Mobilization—Having characterized the use of FRET between CFP- and YFP-tagged PH domains of PLCδ1 to record the effects of PLC activation, we next set out to compare the kinetics of responses to a set of calcium-mobilizing GPCR agonists. Included in this panel were the peptide agonists BK and NKA, as well as the bioactive lipid LPA, the protease thrombin, and the bioactive amine, histamine. Thrombin and LPA, in addition to inducing Ca^{2+} mobilizations from internal stores, are also strong inducers of Rho-dependent remodeling of the actin cytoskeleton in these cells (23, 28). Histamine, on the other hand, does not induce Rho-dependent actin remodeling, but is known to induce Ca^{2+} oscillations in several cell types, *e.g.* Refs. 30 and 31.

These agonists evoke very similar Ca^{2+} mobilizations in N1E-115 cells, characterized by a fast onset and rapid termination well within 2 min (Fig. 6). Estimated peak Ca^{2+} levels ranged from 0.6 to 2 μM, and, again, showed no consistent differences between agonists. When the effects of PLC activation were recorded by FRET analysis, using the same agonists under identical conditions, quite unexpectedly several distinct kinetic profiles were obtained (Fig. 6). First, both NKA and BK caused fast and near complete translocation of the probe. This response was transient, returning to baseline within 2–5 min. Stimulation with thrombin or LPA evoked a different type of response: these translocations had slower onset and smaller amplitude, averaging 25% of BK response control values (n = 22). They also returned to baseline at a slower rate. The response to histamine was much slower and of small amplitude (40% of BK-induced peak values, n = 15), but it was long-lasting (at least for 15 min, but often much longer).

Differences in degree of $PI(4,5)P_2$ hydrolysis induced by activation of different G_q-coupled receptors have also been reported (15, 32) in biochemical studies. However, so far only cytosolic Ca^{2+} responses could be used to analyze receptor activation patterns at the single cell level. On the other hand, the shape of the Ca^{2+} response is determined by several other factors: it can be triggered at relatively low levels of IP_3 and its shape is also determined by the Ca^{2+}-induced Ca^{2+} release and inactivation properties of the IP_3-receptor channels, as well as by the activities of the various Ca^{2+} sequestration mechanisms. The present approach provides an opportunity to study a more upstream receptor-mediated event, namely PLC activation, and its regulation in detail at the single cell level.

PH Domain Translocation Kinetics Mirror Receptor Activation—These results thus suggest that PLC activation as assessed by FRET is a more faithful index of receptor activity than the more distal Ca^{2+} transients. However, inactivation could occur at various steps in the signal cascade, including at the levels of receptor, G protein, and PLC and, conceivably, also by modulation (up-regulation) of $PI(4,5)P_2$ resynthesis. To test whether there is desensitization at the level of PLC, G proteins

were directly activated using AlF^{4-} (Fig. 7*A*). While the onset of ALF^{4-}-induced translocation was slow, no desensitization was observed in any of these experiments. Similarly, when viewed using confocal microscopy, cells expressing a constitutively active $G\alpha_q$ mutant showed mostly cytosolic localization of PLCδ1PH-GFP domains for at least 2 days (Fig. 7*B*). Cells transfected with activated $G\alpha_{12}$, which does not activate PLC, showed normal membrane localization of PLCδ1PH-GFP and agonists could still induce translocation of the fluorescence to the cytosol. At lower expression levels, the activating mutant $G\alpha_q$ induced sustained partial translocation that also persisted for several days. These experiments suggested that no significant desensitization occurs downstream of G_q and PLC. In line with this notion, we did not observe significant heterologous desensitization between sequentially added agonists (compare *e.g.* Fig. 4 and 6, *last panel*), whereas prolonged exposure of cells to each individual agonist induced complete (homologous) desensitization.

To further determine whether the membrane association of PLCδ1PH as assessed by FRET truly reports on receptor activity (*i.e.* the coupling and uncoupling between receptors and G proteins), we compared the responses of N1E-115 cells expressing either the wild-type NK2 receptors or a C-terminal truncated form, which is greatly impaired in its ability to desensitize (33). As shown earlier, after stimulation of the wild-type human NK2 receptors the translocation response decays toward baseline within minutes (average 50% recovery time 83 ± 38 s, $n = 25$; compare Fig. 6 and 7*C*). Application of short pulses of the agonist using a puffer pipette resulted in an incomplete desensitization of the translocation response as shown by the small decrease of the peak amplitudes. These individual responses decayed significantly faster (45 ± 7 s, $n = 60$, Fig. 7*C*) between applications of stimuli than the response to a sustained stimulation, reflecting the rapid dissociation of the ligand from the receptor (34). In contrast, stimulation of a C-terminal truncated mutant human NK2 receptor, that was reported to be transforming in Rat-1 fibroblasts, and which has been found to display prolonged coupling to PLC (33, 35, 36), induced a prolonged cytosolic translocation as assessed by our FRET analysis (Fig. 7*C*). However, remarkably, in the majority of cells, the FRET signal eventually slowly returned to baseline (Fig. 7*D*; note the different time scale), with an average 50% recovery time of 1365 ± 599 s ($n = 19$) in the truncated receptor. This finding indicates the existence of an alternative and much slower desensitization mechanism that functions even in NK2 receptors that lack the C terminus. The kinetics of this slow desensitization closely paralleled those of receptor internalization (not shown), suggesting that one of the main determinants for termination of NKA-induced PLC signaling could be receptor internalization. Analysis of receptor activity by monitoring PLC activity by FRET will greatly aid further studies addressing these questions in more detail.

In summary, in the present study, we describe a fluorescence resonance-based detection scheme to follow the membrane localization of tagged PLCδ1 PH domains for analysis of activation-inactivation kinetics of PLC in single cells with high temporal resolution. This method can be used at comparable expression levels of the PH domains that are used for confocal detection, but has a number of significant advantages over the latter. These include: (i) a significant decrease in excitation intensity allowing prolonged experiments or very fast sampling with little phototoxicity and photobleaching; (ii) suitability for very flat cells such as fibroblasts and motile cells; (iii) extendibility to record from cell populations as well as from small subregions such as neurites; and (iv) a simpler detection hardware. The FRET assay produces a fairly robust response that can be routinely obtained in a variety of cell types.

Our analysis of the translocation responses suggests that localization of PLCδ1PH-GFP mainly reports on $PI(4,5)P_2$ dynamics, although at high concentrations IP_3 can also contribute to translocation of the PH domains to the cytosol. Comparison of the Ca^{2+} and FRET-recorded responses of several agonists of GPCRs suggests that detecting PLCδ1PH translocation by FRET provides a more faithful reflection of receptor activity than the Ca^{2+} signal and that little if any "desensitization" or "uncoupling" occurs beyond the level of G proteins. FRET analysis should be a very useful tool not only to explore the activation patterns of PLC in individual cells but also for the dissection of various mechanisms of receptor desensitization.

Acknowledgments—We thank Drs. W. Moolenaar, N. Divecha, J. Hallstead (Department of Biochemistry), and members of the Department of Cell Biology for discussions and comments on the manuscript, and Dr. F. Postma for comments and help with the figures. We also thank Drs. T. Meyer, J. Alblas, O. Kranenburg, A. Miyawaki, and R. Y. Tsien for plasmids.

REFERENCES

1. Thomas, A. P., Bird, G. S., Hajnoczky, G., Robb-Gaspers, L. D., and Putney, J. W., Jr. (1996) *FASEB J.* **10,** 1505–1517
2. Dupont, G., and Goldbeter, A. (1998) *Bioessays* **20,** 607–610
3. Chau, L. Y., Lin, T. A., Chang, W. T., Chen, C. H., Shue, M. J., Hsu, Y. S., Hu, C. Y., Tsai, W. H., and Sun, G. Y. (1993) *J. Neurochem.* **60,** 454–460
4. Stauffer, T. P., Ahn, S., and Meyer, T. (1998) *Curr. Biol.* **8,** 343–346
5. Varnai, P., and Balla, T. (1998) *J. Cell Biol.* **143,** 501–510
6. Varnai, P., Rother, K. I., and Balla, T. (1999) *J. Biol. Chem.* **274,** 10983–10989
7. Gray, A., Van Der, K. J., and Downes, C. P. (1999) *Biochem. J.* **344,** 929–936
8. Lankiewicz, L., Malicka, J., and Wiczk, W. (1997) *Acta Biochim. Pol.* **44,** 477–489
9. Pollok, B. A., and Heim, R. (1999) *Trends Cell Biol.* **9,** 57–60
10. Kranenburg, O., Poland, M., van Horck, F. P., Drechsel, D., Hall, A., and Moolenaar, W. H. (1999) *Mol. Biol. Cell* **10,** 1851–1857
11. Balla, T., Nakanishi, S., and Catt, K. J. (1994) *J. Biol. Chem.* **269,** 16101–16107
12. Miyawaki, A., Llopis, J., Heim, R., McCaffery, J. M., Adams, J. A., Ikura, M., and Tsien, R. Y. (1997) *Nature* **388,** 882–887
13. Patterson, G. H., Knobel, S. M., Sharif, W. D., Kain, S. R., and Piston, D. W. (1997) *Biophys. J.* **73,** 2782–2790
14. Tilly, B. C., van Paridon, P. A., Verlaan, I., de Laat, S. W., and Moolenaar, W. H. (1988) *Biochem. J.* **252,** 857–863
15. van der Bend, R. L., de Widt, J., van Corven, E. J., Moolenaar, W. H., and van Blitterswijk, W. J. (1992) *Biochem. J.* **285,** 235–240
16. Zhang, C., Schmidt, M., Eichei-Streiber, C., and Jakobs, K. H. (1996) *Mol. Pharmacol.* **50,** 864–869
17. Wijelath, E. S., Kardasz, A. M., Drummond, R., and Watson, J. (1988) *Biochem. Biophys. Res. Commun.* **152,** 392–397
18. Divecha, N., Banfic, H., and Irvine, R. F. (1991) *EMBO J.* **10,** 3207–3214
19. Stephens, L., Jackson, T. R., and Hawkins, P. T. (1993) *Biochem. J.* **296,** 481–488
20. Myers, D. E., and Larkins, R. G. (1989) *Cell Signal.* **1,** 335–343
21. Tsien, R. Y. (1998) *Annu. Rev. Biochem.* **67,** 509–544
22. Tall, E. G., Spector, I., Pentyala, S. N., Bitter, I., and Rebecchi, M. J. (2000) *Curr. Biol.* **10,** 743–746
23. Jalink, K., Eichholtz, T., Postma, F. R., van Corven, E. J., and Moolenaar, W. H. (1993) *Cell Growth & Differ.* **4,** 247–255
24. van Leeuwen, F. N., van Delft, S., Kain, H. E., van der Kammen, R. A., and Collard, J. G. (1999) *Nat. Cell Biol.* **1,** 242–248
25. Hirose, K., Kadowaki, S., Tanabe, M., Takeshima, H., and Iino, M. (1999) *Science* **284,** 1527–1530
26. Wiedemann, C., Schafer, T., and Burger, M. M. (1996) *EMBO J.* **15,** 2094–2101
27. Hunyady, L., Merelli, F., Baukal, A. J., Balla, T., and Catt, K. J. (1991) *J. Biol. Chem.* **266,** 2783–2788
28. Jalink, K., and Moolenaar, W. H. (1992) *J. Cell Biol.* **118,** 411–419
29. Lemmon, M. A., Ferguson, K. M., O'Brien, R., Sigler, P. B., and Schlessinger, J. (1995) *Proc. Natl. Acad. Sci. U. S. A.* **92,** 10472–10476
30. Paltauf-Doburzynska, J., Frieden, M., Spitaler, M., and Graier, W. F. (2000) *J. Physiol.* **524,** 701–713
31. Zhu, D. M., Tekle, E., Huang, C. Y., and Chock, P. B. (2000) *J. Biol. Chem.* **275,** 6063–6066
32. Tilly, B. C., Tertoolen, L. G., Lambrechts, A. C., Remorie, R., de Laat, S. W., and Moolenaar, W. H. (1990) *Biochem. J.* **266,** 235–243
33. Alblas, J., van Etten, I., Khanum, A., and Moolenaar, W. H. (1995) *J. Biol. Chem.* **270,** 8944–8951
34. Vollmer, J. Y., Alix, P., Chollet, A., Takeda, K., and Galzi, J. L. (1999) *J. Biol. Chem.* **274,** 37915–37922
35. Alblas, J., van Etten, I., and Moolenaar, W. H. (1996) *EMBO J.* **15,** 3351–3360
36. Alblas, J., van Corven, E. J., Hordijk, P. L., Milligan, G., and Moolenaar, W. H. (1993) *J. Biol. Chem.* **268,** 22235–22238
37. Miyawaki, A., Llopis, J., Mizuno, H., Jalink, K., and Tsien, R. (2000) *Calcium Signaling: A Practical Approach*, pp. 3–16, Oxford University Press, Oxford, in press